

# Impacts of $\text{Eu}^{2+}$ -doped $\text{K}_3\text{LuSi}_2\text{O}_7$ phosphor and a scattering particle on conventional white light emitting diodes

Le Doan Duy<sup>1</sup>, Nguyen Le Thai<sup>2</sup>, Pham Hong Cong<sup>3</sup>, Thinh Cong Tran<sup>4</sup>

<sup>1</sup>Faculty of Basic Sciences, Vinh Long University of Technology Education, Vinh Long Province, Vietnam

<sup>2</sup>Faculty of Engineering and Technology, Nguyen Tat Thanh University, Ho Chi Minh City, Vietnam

<sup>3</sup>Faculty of Electrical Engineering Technology, Industrial University of Ho Chi Minh City, Ho Chi Minh City, Vietnam

<sup>4</sup>Faculty of Electrical and Electronics Engineering, Ton Duc Thang University, Ho Chi Minh City, Vietnam

## Article Info

### Article history:

Received Oct 10, 2023

Revised Feb 19, 2024

Accepted Mar 28, 2024

### Keywords:

$\text{CaCO}_3$

$\text{K}_3\text{LuSi}_2\text{O}_7$

LEDs

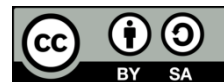
Mie scattering

YAG:Ce

## ABSTRACT

The  $\text{K}_3\text{LuSi}_2\text{O}_7$  phosphor doping  $\text{Eu}^{2+}$  rare-earth ions (KLS:Eu) was reported to possess broad emission band from near-ultraviolet to near-infrared. Additionally, this phosphor showed a wide absorption band of 250-600 nm, allowing it to be excited by blue-light chip of 460 nm, making it one of the suitable phosphor materials for a light emitting diode (LED). Besides, the scattering particle material  $\text{CaCO}_3$  is incorporated into the yellow phosphor layer to serve the scattering-enhancement purpose. The combination of both materials aims at accomplishing improvements in performance of commercial LED package. The concentration of KLS:Eu is constant while that of  $\text{CaCO}_3$  is modified. As a result, the scattering factor is regulated and become the key factor influencing the optical outputs of the simulated LED. The increasing  $\text{CaCO}_3$  concentration enhances the phosphor scattering efficiency of light, helping to improve the lumen output and color-temperature consistency of the LED. However, the color rendering performance declines as a function of the  $\text{CaCO}_3$  growing amount, despite the presence of a KLS:Eu phosphor layer. Further works should be done to optimize the application of KLS:Eu in cooperation with scattering particles for a higher-quality LED device.

*This is an open access article under the [CC BY-SA](https://creativecommons.org/licenses/by-sa/4.0/) license.*



## Corresponding Author:

Thinh Cong Tran

Faculty of Electrical and Electronics Engineering, Ton Duc Thang University

Ho Chi Minh City, Vietnam

Email: tranconghinh@tdtu.edu.vn

## 1. INTRODUCTION

The light emitting diodes (LEDs) of solid-state lighting sources which broad emission bands have been utilized in many fields such as commercial and industrial lighting, display, transportation, medical and biological solutions [1], [2]. The reasons making LEDs popular can include compactness, mercury-free production, long-time services, and low heat dissipation, compared to the conventional halogen light. To fabricate a package of LED, it commonly uses the cooperation of single or multiple phosphor materials and a blue, near-ultraviolet, or near-infrared chip cluster, depending on the application requirements [3]–[5]. This type of LED is also known as phosphor-converted LEDs. The conventional commercial LED utilized the YAG:Ce<sup>3+</sup> yellow phosphor and blue-pumped chip to generate white light. The high luminescence of this package was recognized but the color uniformity and rendition were noticeably low as the red spectrum was not presented in the visible wavelength band of the white light. Besides, the phosphor is often degraded due to humidity and heat exposure, leading to shorter service life and decreasing efficiency [6]–[8]. Therefore, investigations on developing phosphors with broadband emissions for high-quality LED modules have been extensively carried out.

Researches have interested in the rare-earth or metal ions, such as  $\text{Pr}^{3+}$ ,  $\text{Nd}^{3+}$ , and  $\text{Tm}^{3+}$  or  $\text{Ni}^{2+}$ , as dopants for inorganic hosts. Nevertheless, the 4f-4f transitions of these rare-earth ion result in sharp but narrow emission while presenting weak absorbance, which does not satisfy the various applications in sensing technology field. Besides, the  $\text{Ni}^{2+}$  metal ion can achieve broadband emission in the near the near-infrared area, however, its efficiency is inferior. Unlike the rare-earth ions with 4f-4f transition, it is possible to obtain high efficacy, broad, and tunable emission with the  $\text{Eu}^{2+}$  owing to its 4f-5d transition. Generally, the crystalline environment of the host material primarily influences the emission energy distribution of the  $\text{Eu}^{2+}$  ions, including the bond lengths, the number of coordination, and the cation symmetries [9]. To get the broader emission band for  $\text{Eu}^{2+}$ -doped phosphors, especially in the near-infrared region for high-efficiency sensing devices, it is essential to strengthen the crystal field splitting and enhance the  $\text{Eu}^{2+}$ -originated centroid shift. A previous study showed that in the red-emission  $\text{Rb}_3\text{YSi}_2\text{O}_7:\text{Eu}^{2+}$ , the  $\text{Eu}^{2+}$  tended to occupy the cation site having small coordination number, leading to large redshift and higher probability of stronger crystal field splitting to achieve the near-infrared emission for the phosphor [10]. Accordingly, when replacing ions  $\text{Y}^{3+}$  and  $\text{Rb}^{3+}$  with smaller ions  $\text{Lu}^{3+}$  and  $\text{K}^+$ , it is possible to further induce the crystal-field-splitting strength [11], [12].

Besides, the commercial LED device confront the low light distribution uniformity as the light concentrated at the center of the LED. This drawback can be attributed to the inferior scattering of incident and converted light, leading to high color temperature of the generated white light, limiting the utilization of the LED device in general lighting aspects. The scattering factor plays a critical role in the angular uniformity of light distribution, which is a desirable property to diminish the yellow-ring phenomenon [13]. Among various methods of enhancing scattering of the phosphor layer, using the scattering particles caught significant attention from researchers. Articles presented that the  $\text{CaCO}_3$  particle is the one inducing the greatest luminous flux of the phosphor-converted LED compared to other scattering particles such as  $\text{TiO}_2$  or  $\text{CaF}_2$  [14], [15]. Henceforth, this paper utilizes the  $\text{Eu}^{2+}$ -doped  $\text{K}_3\text{LuSi}_2\text{O}_7$  (KLS:Eu) for the commercial LED fabrication and  $\text{CaCO}_3$  particle for scattering regulation. The effects of KLS:Eu phosphor and  $\text{CaCO}_3$  material on the transmission power, scattering events, luminous and chromatic properties of the prepared LED are investigated and demonstrated. It indicates that the KLS:Eu phosphor can contribute to enhancing the yellow-to-orange emission band of the LED and high dosage of  $\text{CaCO}_3$  can improve the conversion of blue light from yellow-red light of the phosphor layers. The luminous strength of the LED and the color-temperature consistency of the LED show improvements, but the chromatic rendition is lowered when the concentration of  $\text{CaCO}_3$  increases and of KLS:Eu phosphor is constant. The phosphor and scattering particle are promising for LED model require improved luminous efficiency and color uniformity.

## 2. METHOD

The phosphor KLS:Eu was synthesized via the solid-state reaction route consisting a high-temperature (1,350 degrees Celsius) sintering phase in 80% $\text{N}_2$ /20% $\text{H}_2$  atmosphere. The materials for the synthesis include  $\text{K}_2\text{CO}_3$ ,  $\text{Lu}_2\text{O}_3$ ,  $\text{SiO}_2$ , and  $\text{Eu}_2\text{O}_3$ , all of which are grounded and mixed stoichiometrically. The sintering phase was conducted with the mixture in an alumina crucible for 6 hours. The obtained product was cooled down to room temperature for the next investigations. The LED structure using KLS:Eu phosphor is shown in Figure 1. The real model of the prepared LED is presented in Figure 1(a). The remote phosphor structure was applied for incorporating the red phosphor and  $\text{CaCO}_3$  particles to optimize the luminous output of the LED, as depicted in Figure 1(b). The  $\text{CaCO}_3$  particles was incorporated into the yellow phosphor layer with the concentration ranging from 0 wt% to 50 wt%. The KLS:Eu phosphor concentration was fixed, and the layer did not include  $\text{CaCO}_3$  particle. Figure 1(c) is the 3D simulation obtained using the LightTools software version 9.0. Figure 1(d) depicts the LED chip cluster in which the utilized chips have radiant flux of 1.6 W and blue emission centering at around 460 nm [16]. The photoluminescence spectra of the LED device with  $\text{CaCO}_3$  and KLS:Eu phosphor were collected using the NOVA fiber fiber spectrophotometer with 460 nm blue-chip excitation source. The stability and robustness of the phosphor when using in the LED is crucial as the internal temperature of the LED can reach 100 °C. The phosphor was tested under 80 °C and exhibited good chemical stability as the  $\text{Eu}^{2+}$  was barely changed to the  $\text{Eu}^{3+}$  after a long exposure. Besides, when the heat was increased from room temperature to more than 100 °C, the luminescence intensity of the phosphor decrease, by about 41% when temperature arrived to 150 °C. The thermal quenching effect may be attributed to this phenomenon, which can be examined using the thermal activating energy ( $E_a$ ) based on Dorenbos work [17]:

$$E_a = \frac{T_{qc}}{680} eV \quad (1)$$

Where  $T_{qc}$  represents the thermo-quenching temperature. The thermo-quenching temperature is the temperature when emission intensity is about 50% of the room-temperature intensity. On the increasing of temperature, the blue shift in the emission peaks of the KLS:Eu phosphor was observed. This can be ascribed to the larger crystal field splitting of  $\text{Eu}^{2+}$  in  $\text{K}^+$  and Lu sites causing the smaller  $E_a$  values. Thus, as the heat increases, the phosphor emission intensity at shorter wavelengths is stronger. The KLS:Eu phosphor can be well excited by the blue-chip excitation (460 nm) as its absorption band was obtained in a wide region of 250-600 nm owing to the 4f-5d transition of  $\text{Eu}^{2+}$  ions occupied K and Lu sites in the  $\text{K}_3\text{LuSi}_2\text{O}_7$  host. Additionally, with this wide-band absorption, the phosphor can exhibit deep red color when observing under natural light. This implies that the phosphor can provides the red spectra for the white light [18].

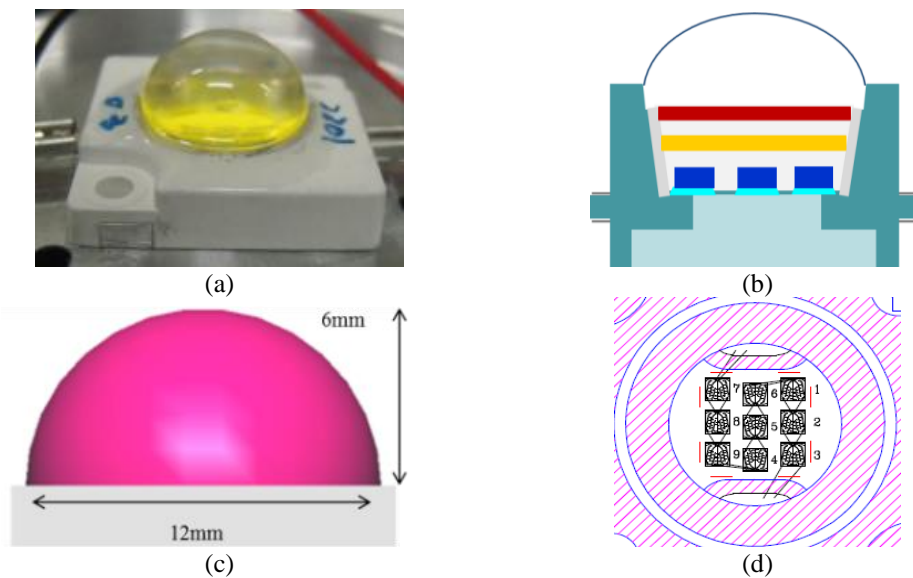


Figure 1. Commercial LED model: (a) photo of a prepared LED package, (b) cross-section of the LED package, (c) simulation model by LightTools software, and (d) the chip cluster in the LED

### 3. RESULTS AND DISCUSSION

The transmission spectra of LED in the presence of the KLS:Eu phosphor can be seen in Figure 2, in which the concentration of  $\text{CaCO}_3$  varies in a range of 0-50 wt%. All the sub figures show two eminent emission peaks centering at  $\sim 460$  nm and  $\sim 560$  nm and a minor peak at around 740 nm. These peaks could be emerged from the blue chips, the YAG:Ce phosphors, and the KLS:Eu phosphor, respectively. The insignificant peak at 740 nm in the emission range indicates that the KLS:Eu is somehow activated by the blue radiation from the LED chips but does not contribute much to the formation of white light. This can be attributed to the arrangement of phosphor layer in the simulation, in which the KLS:Eu is above the YAG:Ce/ $\text{CaCO}_3$  phosphor layer. Such an arrangement could limit the LED-chip blue light interacting directly with the second phosphor layer, leading to the weaker emission.

On the increase of  $\text{CaCO}_3$ , there is no shift noticed in the emission band but the intensity. As the added amount of  $\text{CaCO}_3$  increases, the intensity of the 460-nm peaks declines while that of the 560-nm peak increases. With  $\text{CaCO}_3$  concentration of 10 wt%, the peak intensity does not change much, featuring that the 460-nm peak is greater than the 560-nm one. When the dosage of  $\text{CaCO}_3$  reaches 30-35 wt%, two peaks are relatively equivalent. However, as  $\text{CaCO}_3$  amount is beyond 35 wt%, the 460-nm peak starts to decline while the 560-nm noticeably increases, indicating the more effective blue-light utilization in the LED package. In other words, the observed increase in the yellow-orange region (520-590 nm) can be attributed to the efficient light conversion of the yellow phosphor YAG:Ce phosphor with higher  $\text{CaCO}_3$  concentrations. On the other hand, with the addition of  $\text{CaCO}_3$  particles, the concentration of YAG:Ce phosphor must be adjusted to support the stability of color temperature. Figure 3 shows the decline in YAG:Ce phosphor amount in response to the increase in showing the potential of  $\text{CaCO}_3$  dosage. This decrease also attributed to the luminescence peak (560 nm) observed in green region [19].

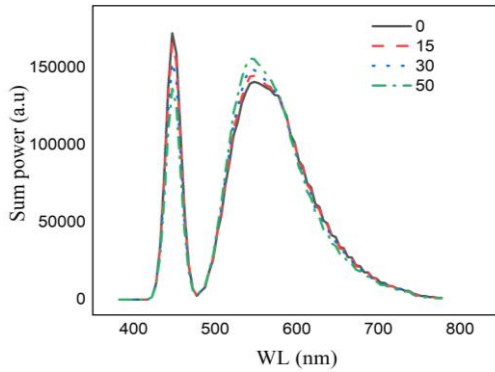


Figure 2. Transmission spectra as a function of increasing  $\text{CaCO}_3$  amount in the presence of KLS:Eu phosphor layer

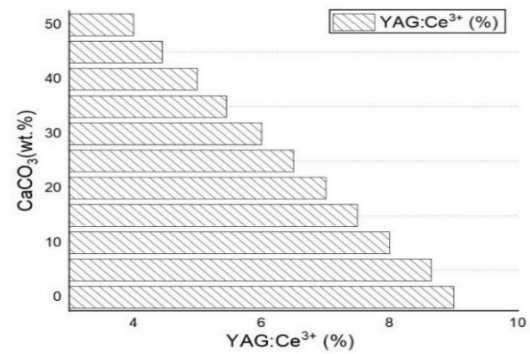


Figure 3. The reduction of YAG:Ce concentration as a function of increasing  $\text{CaCO}_3$  amount

The change in the emission peaks' intensities when adding KLS:Eu phosphor with different amounts can be induced by the change in scattering performance of the light in LED package. We determined the scattering coefficients (SCs) and reduced scattering coefficients (RSCs) of the LED to see the effect of  $\text{CaCO}_3$  amount on the scattering efficiency, as shown in Figures 4 and 5, respectively. In Figure 4, the SCs increases gradually when the  $\text{CaCO}_3$  concentration increases gradually by a small of 5 wt% in each case (from 5-25 wt%, as shown in Figure 4(a)). However, as the  $\text{CaCO}_3$  amount significantly surges to 50 wt%, the SCs value also grows noticeable, showing about 12.5 times greater than that with  $\text{CaCO}_3$  amount at 5 wt% as shown in Figure 4(b). In terms of the RSCs, the increase between 5-15 wt%  $\text{CaCO}_3$  is not much, just about  $0.12 \text{ mm}^{-1}$  in each case as shown in Figure 5(a). However, the difference in RSCs becomes larger as the  $\text{CaCO}_3$  amount increases further, especially at 380 nm wavelength, reaching 3 times and 6 times larger with  $\text{CaCO}_3$  amount of 30 wt% as shown in Figure 5(a) and 50 wt% Figure 5(b) respectively. The introduction of  $\text{CaCO}_3$  particle generally increase the scattering performance as all values go upward as the phosphor concentration increases [20]–[22]. Such phenomena help promote the forward scattering and conversion effectiveness of blue light. However, when the  $\text{CaCO}_3$  increases, more blue light will be observed and converted into yellow light, so the intensity of the blue (460 nm) peak tends to decrease while that of the yellow (560 nm) peak is supplemented.

The luminous performance of the blue-pumped LED when using different amounts of  $\text{CaCO}_3$  is demonstrated in Figure 6. Interestingly, the luminous flux intensity becomes stronger as the concentration of  $\text{CaCO}_3$  increases, showing the potential of  $\text{CaCO}_3$  in achieving better light extraction efficiency for the remote phosphor structure. Meanwhile, the color rendering index (CRI) decreases with the increasing dosage of  $\text{CaCO}_3$  scattering particle, as shown in Figure 7. Referring to Figure 2, the presence of KLS:Eu phosphor does not contribute much to enhancing the visible red spectrum as it exhibits the emission peak at 740 nm in the near-infrared range. The high visible red-light energy is the key to significantly improved CRI value of the white LED. As a result, though the  $\text{CaCO}_3$  at higher amount increase the scattering of blue light and better light conversion by the phosphors, the lack of visible red spectrum is not addressed to get higher CRI for the as-prepared LED.

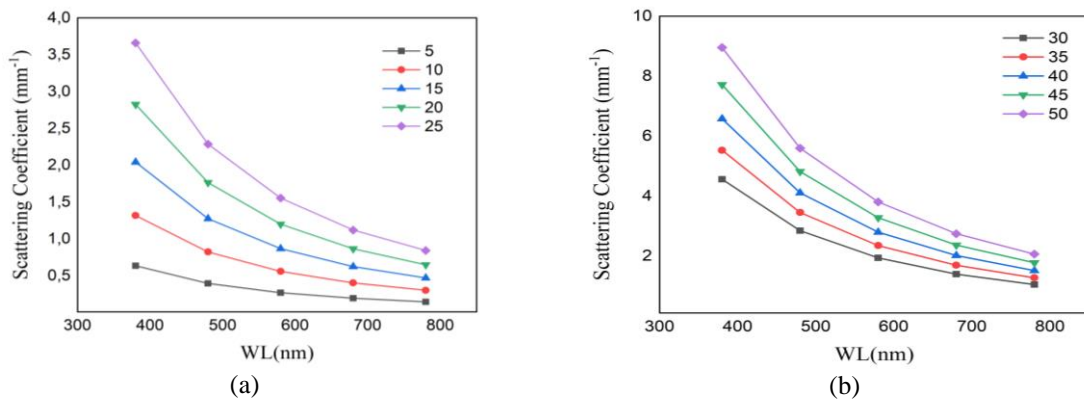


Figure 4. Scattering coefficients as a function of increasing  $\text{CaCO}_3$  amount (a)  $\text{CaCO}_3$  by 5-25% and (b)  $\text{CaCO}_3$  by 5%

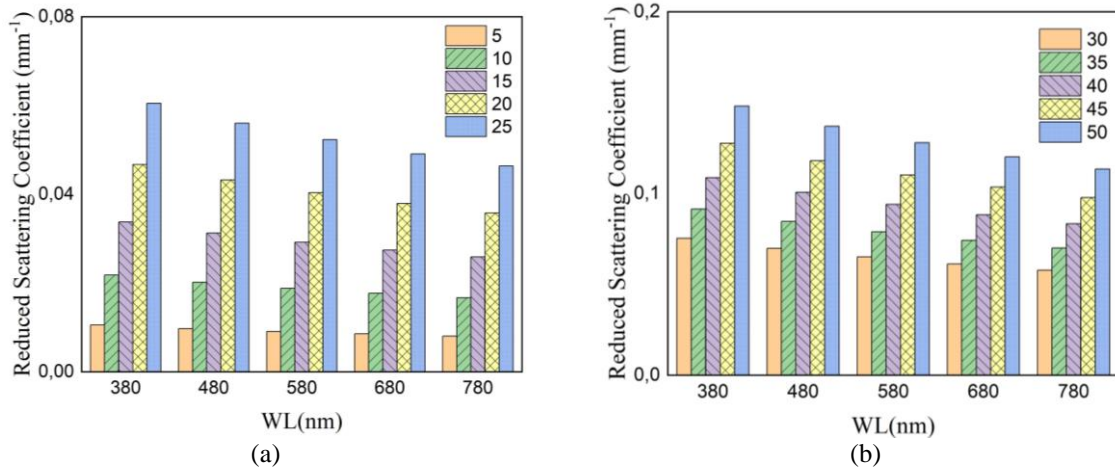


Figure 5. Reduced scattering coefficients as a function of increasing  $\text{CaCO}_3$  amount (a)  $\text{CaCO}_3$  by 30% and (b)  $\text{CaCO}_3$  by 50%

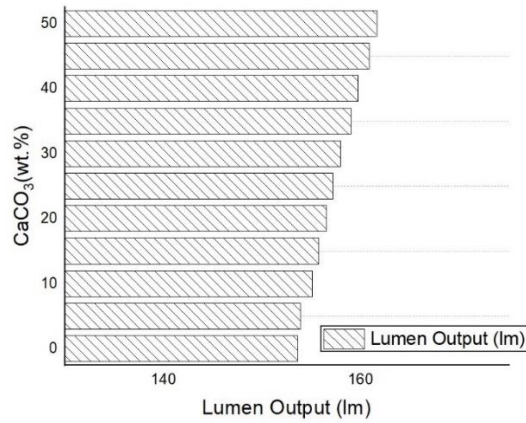


Figure 6. The LED lumen output as a function of increasing  $\text{CaCO}_3$  amount

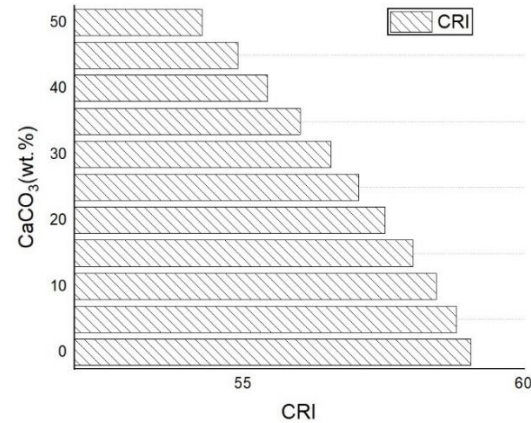


Figure 7. The CRI as a function of increasing  $\text{CaCO}_3$  amount in the presence of KLS:Eu phosphor layer

To verify the decline of color rendition in the presence of  $\text{CaCO}_3$ , we calculate the color quality scale (CQS), which is a newer color-evaluation parameter for LED light. The CQS can assess critical categories to give a more accurate result. Those categories include CRI, color coordination, and visual preferences of subjects. When the  $\text{CaCO}_3$  is introduced and its concentration increases, the CQS values in Figure 8 gradually drop, which further confirm the insufficient red component in the visible white-light emission. The dominant yellow-light amount could be the cause for the CRI and CQS decreases as well as lumen-output increase. The high-intensity luminosity favors the monochromatic light as well as high blue-light emission. On the other hand, the high color-rendering performance requires broad band emission with sufficient red-light energy to give the optimal chromatic fidelity [23], [24]. Therefore, the KLS:Eu addition at high concentrations leads to the enhancement in the LED's lumen output and the decline in CQS and CRI. Such findings also imply the improvement in color-temperature uniformity of the LED when using  $\text{CaCO}_3$  with high amount in combination with KLS:Eu phosphor layer. The angular color temperature (A-CCT) and color deviation (D-CCT) as a function of increasing KLS:Eu concentration can be observed in Figures 9 and 10, respectively [25]. Overall, at  $0^\circ$  viewing angle, the A-CCT gradually declines when the concentration of KLS:Eu increases. Additionally, the D-CCT in cases of high KLS:Eu concentration is generally lower compared to that when KLS:Eu concentration is at 0 wt%. The lowest D-CCT is recorded with 35 wt% KLS:Eu. These results demonstrate the ability to enhance the luminous performance and reduce the D-CCT to get better color-temperature uniformity. It also indicates the need to modify the KLS:Eu compound to achieve stronger red-emission energy for the LED package require excellent color rendering efficiency.



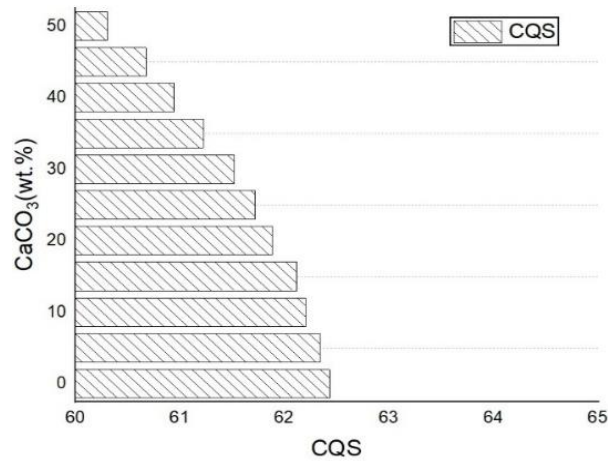


Figure 8. The CQS as a function of increasing CaCO<sub>3</sub> amount

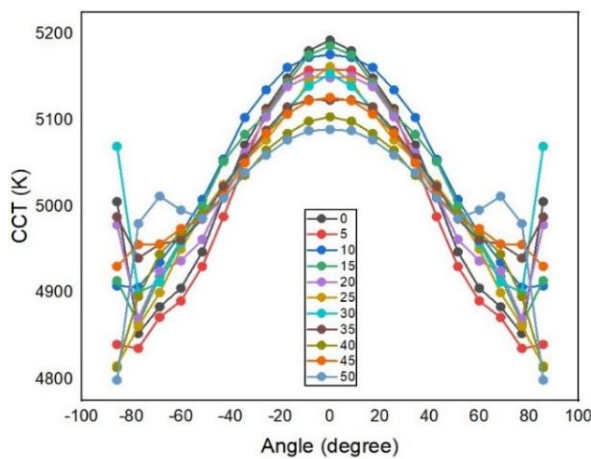


Figure 9. The angular CCT as a function of increasing CaCO<sub>3</sub> amount

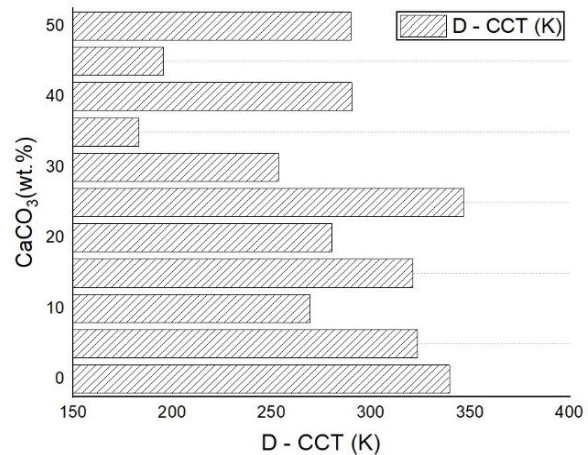


Figure 10. The CCT deviation as a function of increasing CaCO<sub>3</sub> amount

#### 4. CONCLUSION

The paper used Eu<sup>2+</sup>-doped K<sub>3</sub>LuSi<sub>2</sub>O<sub>7</sub> phosphor and CaCO<sub>3</sub> scattering particles in commercial LED package to get improvements in the performance. The concentration of KLS:Eu is constant while that of CaCO<sub>3</sub> is modified as a mean to regulate the scattering factor of the as-prepared LED's remote phosphor structure. On the increasing CaCO<sub>3</sub> concentration, the scattering efficiency of light enhances, allowing to achieve better blue-light utilization by the phosphor layer. As a result, the lumen output and color-temperature consistency of the LED improve with higher CaCO<sub>3</sub> amounts. However, the CRI and CQS performances decrease in response to the higher amount of CaCO<sub>3</sub>, despite the presence of a KLS:Eu phosphor layer. For a higher-quality LED device and a wider application range of the phosphor-converted LED, further works should be done to optimize the application of KLS:Eu in cooperation with scattering particles, such as structure re-arrangement or phosphor compound modification.





#### REFERENCES

- [1] P. S. Sengar, T. K. Rawat, and H. Parthasarathy, "Color image enhancement by scaling the discrete wavelet transform coefficients," Jun. 2013, doi: 10.1109/AICERA-ICMiCR.2013.6575994.
- [2] Y. Huang, X. Meng, and L. Li, "No-reference quality prediction for DIBR-synthesized images using statistics of fused color-depth images," in *Proceedings - 3rd International Conference on Multimedia Information Processing and Retrieval, MIPR 2020*, Aug. 2020, pp. 135–138, doi: 10.1109/MIPR49039.2020.00035.
- [3] X. Yue, D. Miao, Y. Wu, C. Zhong, and Y. Chen, "Scale selection in roughness based color quantization," in *Proceedings - 2013 IEEE International Conference on Granular Computing, GrC 2013*, Dec. 2013, pp. 412–417, doi: 10.1109/GrC.2013.6740446.




- [4] X. Zhang, "A novel color image fusion method based on the multi-scale Retinex and DWT," in *Proceedings - 2009 International Conference on Information Management and Engineering, ICIME 2009*, 2009, pp. 395–398, doi: 10.1109/ICIME.2009.29.
- [5] C. Charrier and H. Cherifi, "Quantifying perceptual image quality by difference scaling," in *6th International Symposium on Signal Processing and Its Applications, ISSPA 2001 - Proceedings; 6 Tutorials in Communications, Image Processing and Signal Analysis*, 2001, vol. 2, pp. 422–425, doi: 10.1109/ISSPA.2001.950170.
- [6] S. W. Lee and H. Nam, "A new dithering algorithm for higher image quality of liquid crystal displays," *IEEE Transactions on Consumer Electronics*, vol. 55, no. 4, pp. 2134–2138, Nov. 2009, doi: 10.1109/TCE.2009.5373779.
- [7] D. Kim, K. Jung, B. Ham, Y. Kim, and K. Sohn, "Normalized tone-mapping operators for color quality improvement in 3DTV," in *Proceedings of the 2014 9th IEEE Conference on Industrial Electronics and Applications, ICIEA 2014*, Jun. 2014, pp. 430–435, doi: 10.1109/ICIEA.2014.6931201.
- [8] M. C. Ionita, P. Corcoran, and V. Buzuloiu, "On color texture normalization for active appearance models," *IEEE Transactions on Image Processing*, vol. 18, no. 6, pp. 1372–1378, Jun. 2009, doi: 10.1109/TIP.2009.2017163.
- [9] H. Shao, X. Cao, and G. Er, "Objective quality assessment of depth image based rendering in 3DTV system," May 2009, doi: 10.1109/3DTV.2009.5069619.
- [10] I. Petrinska, "Investigation of the color rendering of LED luminaires for human centric lighting," Sep. 2021, doi: 10.1109/Lighting49406.2021.9599086.
- [11] H. B. Kekre and S. D. Thepade, "Improving color to gray and back using Kekre's LUV color space," in *2009 IEEE International Advance Computing Conference, IACC 2009*, Mar. 2009, pp. 1218–1223, doi: 10.1109/IADCC.2009.4809189.
- [12] I. Pekkuksken and Y. Altumbasak, "Directional color filter array interpolation based on multiscale color gradients," in *ICASSP, IEEE International Conference on Acoustics, Speech and Signal Processing - Proceedings*, May 2011, pp. 997–1000, doi: 10.1109/ICASSP.2011.5946574.
- [13] J. S. Li, Y. Tang, Z. T. Li, X. R. Ding, L. S. Rao, and B. H. Yu, "Effect of quantum dot scattering and absorption on the optical performance of white light-emitting diodes," *IEEE Transactions on Electron Devices*, vol. 65, no. 7, pp. 2877–2884, Jul. 2018, doi: 10.1109/TED.2018.2830798.
- [14] T. C. Tran, N. D. Q. Anh, and N. T. P. Loan, "Comparison of calcium carbonate and titania particles on improving color homogeneity and luminous flux of WLEDs," *Telkomnika (Telecommunication Computing Electronics and Control)*, vol. 18, no. 5, pp. 2690–2695, Oct. 2020, doi: 10.12928/TELKOMNIKA.v18i5.13552.
- [15] N. T. P. Loan and N. D. Q. Anh, "Utilizing CaCO<sub>3</sub>, CaF<sub>2</sub>, SiO<sub>2</sub>, and TiO<sub>2</sub> particles to enhance color homogeneity and luminous flux of WLEDs," *International Journal of Electrical and Computer Engineering*, vol. 10, no. 5, pp. 5175–5182, Oct. 2020, doi: 10.11591/IJECE.V10I5.PP5175-5182.
- [16] B. Zhang, P. V. Sander, and A. Bernak, "Gradient magnitude similarity deviation on multiple scales for color image quality assessment," in *ICASSP, IEEE International Conference on Acoustics, Speech and Signal Processing - Proceedings*, Mar. 2017, pp. 1253–1257, doi: 10.1109/ICASSP.2017.7952357.
- [17] M. Hanmandlu and D. Jha, "An optimal fuzzy system for color image enhancement," *IEEE Transactions on Image Processing*, vol. 15, no. 10, pp. 2956–2966, Oct. 2006, doi: 10.1109/TIP.2006.877499.
- [18] M. A. Hassan and M. S. Bashraheel, "Color-based structural similarity image quality assessment," in *ICIT 2017 - 8th International Conference on Information Technology, Proceedings*, May 2017, pp. 691–696, doi: 10.1109/ICITECH.2017.8079929.
- [19] Y. Cheng and Y. Wang, "Research on extraction optimization algorithm of color stripe structure based on MATLAB," in *2019 IEEE 3rd International Conference on Electronic Information Technology and Computer Engineering, EITCE 2019*, Oct. 2019, pp. 1208–1211, doi: 10.1109/EITCE47263.2019.9094840.
- [20] T. N. Pappas, "Model-based halftoning of color images," *IEEE Transactions on Image Processing*, vol. 6, no. 7, pp. 1014–1024, Jul. 1997, doi: 10.1109/83.597276.
- [21] S. Agra and A. K. Nisa, "Analyzing the effectiveness of metamorphosing images using color maps," in *Proceedings of the 3rd International Conference on Smart Systems and Inventive Technology, ICSSIT 2020*, Aug. 2020, pp. 1279–1285, doi: 10.1109/ICSSIT48917.2020.9214194.
- [22] W. K. Hu, C. H. Lin, and M. C. Shie, "An economic color printing algorithm using approximate-K," in *Proceedings of the International Symposium on Consumer Electronics, ISCE*, Jun. 2011, pp. 379–383, doi: 10.1109/ISCE.2011.5973853.
- [23] W. Yang *et al.*, "Photometric optimization of color temperature tunable quantum dots converted white LEDs for excellent color rendition," *IEEE Photonics Journal*, vol. 8, no. 5, pp. 1–11, Oct. 2016, doi: 10.1109/JPHOT.2016.2615282.
- [24] N. Doan Quoc Anh, N. Thi Phuong Thao, and M. Voznak, "A novel application of green (La, Ce, Tb)PO<sub>4</sub>:Ce:Tb phosphor on the luminous efficacy and color quality of white LEDs," May 2017, doi: 10.1109/ISNE.2017.7968737.
- [25] T. Al Hagbani, M. T. Nutan, M. A. Veronin, and S. Nazzal, "The utility of colorimetry as a quality control tool for the identification of pharmaceutical tablets," in *2016 32nd Southern Biomedical Engineering Conference (SBEC)*, Mar. 2016, pp. 95–95, doi: 10.1109/sbec.2016.28.

## BIOGRAPHIES OF AUTHORS






**Le Doan Duy**     received the Master degree in physics from Can Tho University, Vietnam. He is working as a lecturer at the Faculty of Basic Sciences, Vinh Long University of Technology Education, Vietnam. His research interests focus on developing the patterned substrate with micro- and nano-scale to apply for physical and chemical devices such as solar cells, OLED, photoanode, theory physics. He can be contacted at email: duyld@vlute.edu.vn.






**Nguyen Le Thai**    received his B.S. in Electronic Engineering from Danang University of Science and Technology, Vietnam, in 2003, M.S. in Electronic Engineering from Posts and Telecommunications Institute of Technology, Ho Chi Minh, Vietnam, in 2011 and Ph.D. degree of Mechatronics Engineering from Kunming University of Science and Technology, China, in 2016. He is currently with the Nguyen Tat Thanh University, Ho Chi Minh City, Vietnam. His research interests include the renewable energy, optimization techniques, robust adaptive control and signal processing. He can be contacted at email: nlthai@ntt.edu.vn.



**Pham Hong Cong**    received his M.S. in Electronic Engineering from Danang University of Science and Technology, Vietnam, in 2010. He is a lecturer at the Faculty of Electrical Engineering Technology, Industrial University of Ho Chi Minh City, Ho Chi Minh City, Vietnam. His research interests are optoelectronics (LED), power transmission and automation equipment. He can be contacted at email: phamhongcong@iuh.edu.vn.



**Thinh Cong Tran**    received the Ph.D. degree in Electrical Engineering from VSB-Technical University of Ostrava, Czech Republic, in 2020. Presently, he is working as a lecturer at the Faculty of Electrical and Electronics Engineering, Ton Duc Thang University, Ho Chi Minh City, Vietnam. His research interests involve the optimization of the power system and applications of soft computing in control of electric machine drives and optics science. He can be contacted at email: trancongthinh@tdtu.edu.vn.